Available online at www.sciencedirect.com
ScienceDirect
Journal of Power Sources 178 (2008) 537–546
JOURNAL OF POWER SOURCES
www.elsevier.com/locate/jpowsour

Percolative model of proton conductivity of Nafion® membranes

Paola Costamagna *, Simone Grosso, Renzo Di Felice

DIChePP, Department of Chemical and Process Engineering 'G.B. Bonino', University of Genoa, Via Opera Pia 15, 16145 Genoa, Italy

Received 18 July 2007; received in revised form 23 September 2007; accepted 24 September 2007
Available online 29 September 2007

Abstract

A model is proposed for the simulation of Nafion® proton conductivity, where it is assumed that proton conduction occurs only in the water present in the membrane pores. Water is considered to be present in the pores due to two different phenomena: adsorption and capillary condensation. In the latter case, the pore is flooded and proton conduction occurs throughout the whole pore section. The conditions under which capillary condensation occurs are simulated in the model through the Kelvin–Cohan equation for condensation. The Kelvin–Cohan equation is a function of RH, temperature and the pore radius; the larger the pore, the higher the RH for which capillary condensation takes place. If the conditions for capillary condensation are not satisfied, then water is present in the pore due to adsorption under the form of a water layer which covers the pore walls and provides a path for proton conduction. In this case, the modified Brunauer–Emmet–Teller (BET) equation has been used in the model to simulate the thickness of the water layer.

In both cases of capillary condensation and adsorption, the conductance g of a pore has then been calculated through the formula $g = \kappa S/l$, where κ is the proton conductivity of water, S the cross-section of the pore volume which is occupied by water, and l is the pore length. Pores of different size are present in the membrane (data of pore size distribution have been extracted from the literature); connectivity of the water layers present in the different pores is necessary in order to achieve a continuous path of proton conduction through the membrane, which is a percolation problem. To this end, the structure of the membrane pores has been simulated in the model through the effective medium approximation (EMA).

The simulation results of proton conductivity of the membrane show good agreement with literature experimental data, even when varying the RH operating conditions.

Keywords: Transport phenomena; Modelling; Nafion®; Percolation theory; Porous materials; Fuel cells

1. Introduction

Nafion® is a perfluorosulphonic acid membrane, originally developed for application in the chloro-alkali process, and now applied in fuel cells, namely proton exchange membrane fuel cells (PEMFCs) and direct methanol fuel cells (DMFCs). Nafion® consists of a perfluorinated polymeric backbone (polytetrafluoroethylene, PTFE) and side chains with SO_3H groups. Several studies have been made in order to understand the nanoscaled structure of Nafion®, since the early work of Gierke et al. [1], who proposed a description, still generally accepted, where the polymeric membrane is pictured in terms of an inverted micellar structure in which the ion exchange sites separate from the fluorocarbon backbone thus forming spherical clusters (pores), which are connected by channels, with the SO_3H groups distributed on the inner surface and pointing inwards (Fig. 1).

When the membrane is humidified, water penetrates the pores, and then, due to their acidic nature, the sulphonic groups dissociate into SO_3^- groups, which remain attached to the backbone chains, and protons, which float in the aqueous phase, and are free to move under the action of an electrical field. Actually, it is ascertained that proton conduction is not occurring through movement of the same proton, but instead by exchange of a free proton (i.e. proton hop) between one H^+–nH_2O cluster and another. The proton hop is preceded by suitable configurational

* Corresponding author. Tel.: +39 010 3532922; fax: +39 010 3532586.
E-mail address: paola.costamagna@unige.it (P. Costamagna).

0378-7753/$ – see front matter © 2007 Elsevier B.V. All rights reserved.
doi:10.1016/j.jpowsour.2007.09.071

Nomenclature

c	parameter in Eq. (5)
C	concentration (mol m^{-3})
EW	equivalent weight (kg kmol^{-1})
g	conductance (Ω^{-1})
g_M	effective network conductance (Ω^{-1})
k	parameter in Eq. (6)
l	pore length (m)
n_T	coordination number
p	pressure (Pa)
p^0	saturation pressure (Pa)
RH	relative humidity
r	pore radius (m)
t	layer thickness (m)
v	pore volume-fraction
V_L	molar volume of bulk liquid (m^3 mol^{-1})
x	specific mass of adsorbed gas (kg kg^{-1})
x_m	specific mass of adsorbed gas in a monolayer (kg kg^{-1})

Greek symbols

γ	surface tension (N m^{-1})
ε	void degree
κ	proton conductivity of water (Ω^{-1} cm^{-1})
λ	moles of water per mole of sulphonic group in membrane
ρ_{memb}	density of dry membrane (kg m^{-3})
σ	molecular diameter (m)
ϕ, ψ	probability density distribution
Λ_m^o	limit molar conductivity (Ω^{-1} m^2 mol^{-1})

polarization fluctuations in water. Subjects of investigation [2,3] have been (i) the size of the typical H^+–nH_2O clusters (H_3O^+, $H_5O_2^+$, $H_9O_4^+$ or a mixture of them) and (ii) the different types of proton conductivity occurring in the middle and on the surface of a water-filled pore. Indeed, in the middle of the water-filled pore, proton conductivity resembles proton conductivity in pure free water, while in proximity of the surface of the pore itself the presence of the SO_3^- groups modifies the proton conduction mechanism. In this respect, Okada et al. [4] demonstrated that some of the water molecules in the membrane are strongly associated with the SO_3^- sites, forming the so-called primary hydration layer present on the pore surface; the ability of these water molecules to form H^+–nH_2O clusters and provide the configurational flexibility necessary in order to contribute to proton conduction is highly compromised, resulting in very low proton conductivity [5].

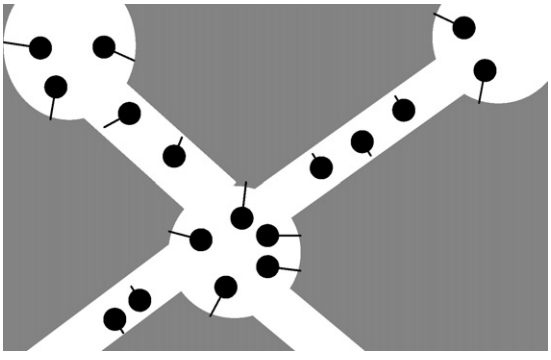

Fig. 1. Structure of pores in Nafion® membranes. (●) Represents the −SO_3H group.

Of course, in order to allow proton conduction, not only must water be present in a pore, but also the aqueous phase must percolate through the membrane, forming a continuous path for proton conduction. Two aspects contribute to the formation of a connected network of water-filled pores inside the membrane, i.e. the amount of water present in the membrane and the structure and pore size distribution of the pore network. Both the previous aspects have been subject of experimental and theoretical studies. In particular, concerning the pore size distribution of the pore network, Divisek et al. [6] have investigated in depth the pore size distribution of Nafion® 117 membranes, by applying a method of standard porosimetry (SPM). According to their results, a wide spectrum of pore diameters was detected, ranging from 1 to 100 nm, with the average value in the order of some nm. Concerning the membrane water content, several experimental studies of the isotherms of water adsorption in Nafion® are reported in the literature. Indeed, the water uptake of Nafion® 117 membranes has been measured by several scientists [7–11]; in all these experiments, water adsorption has been recorded, by suspending dry samples of Nafion® in an inert environment with controlled relative humidity RH (defined as the ratio between the partial pressure of water vapour p and the saturation pressure p^0 at the operating temperature); water uptake is then measured as the difference in weight between the dry state and the state of equilibrium with water vapour. Unfortunately, no studies have examined both adsorption and desorption with the same samples. Indeed, only one study has been found on desorption [6]. The desorption data have been obtained after soaking the membrane in liquid water; during the experiments, the membrane has been kept in a gaseous environment with decreasing values of RH, starting from RH = 1; equilibrium was obtained before recording any data point.

The experimental data obtained by the different authors are reported in Fig. 2. Since the different membranes were not in the same state before the experiments were performed, it is difficult to discuss the differences among the different results in depth. However, it is clear that desorption and adsorption isotherms show hysteretical behaviour. The discrepancy in the values of water impregnation in Nafion® membranes at RH = 1 obtained by soaking the membrane in liquid water or by water adsorption from water vapour at RH = 1 is well known as the Schroeder paradox [9,11,12]. The hysteretical behaviour of Nafion® with hydration/dehydration cycles is also mentioned in other works [5,13]. Generally speaking, hysteresis effects can be explained by the existence of phase transitions [14–16], or by the viscoelastic properties of Nafion® membranes [13], or by the classic vapour–liquid phase transitions, that is capillary condensation in pores with diameters ranging from 1 to 10 nm, which is exactly the pore size of Nafion® as measured experimentally by Divisek

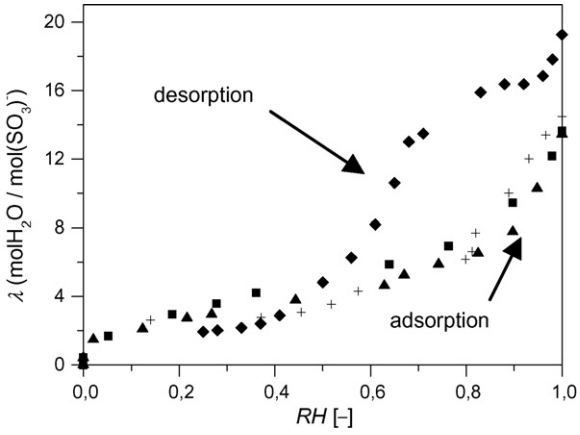

Fig. 2. Experimental literature data of water adsorption and desoption isotherms in Nafion® 117 at 20–30 °C: (▲) adsorption at 25 °C [8]; (■) adsorption at 25 °C [7]; (+) adsorption at 30 °C [9]; (♦) desorption at 20 °C [6].

et al. [6]. In this paper, this latter interpretation is followed and the visco-elastic properties of Nafion® membranes are not taken into account. Thus, we assume that, when starting from a dry membrane and by increasing RH, membrane pore-filling is due to water adsorption on the pore walls coupled to capillary condensation; for each value of RH some of the pores (the smallest ones) are completely filled with water, while the largest pores contain only a thin layer of water adsorbed on their pore surface. Thus, the conductance of each pore is thus very different depending on its radius, and the overall conductivity of the membrane depends on the percolation through the pore network.

In this paper, a model of Nafion® membranes is proposed, which, starting from the pore size distribution proposed by Divisek et al. [6], evaluates the occurrence of capillary condensation in the pores of the membrane, calculates their proton conductance, and finally the overall proton conductivity of the membrane taking into account percolation within the pore network through the effective medium approximation. Each of these aspects will be illustrated in more detail in Section 2. Section 3 includes a comparison between model results and literature experimental data of water adsorption and proton conductivity of Nafion® 117 membranes at 20 °C and at different values of RH. Indeed, literature studies [17] have demonstrated that not only the water uptake, but also the proton conductivity of Nafion® shows a dramatic dependence upon the operating conditions of relative humidity (RH), with several orders of magnitude of difference between the values obtained at 10–20% RH and at 100% RH (where maximum conductivity is achieved). This is a significant issue for fuel cell applications, since any zone of the fuel cell where the relative humidity is low shows a dramatic loss of performance. However, we should point out that there is a difference in the operating conditions of a Nafion® membrane when operating as the electrolyte in a PEMFC, and the Nafion® membrane simulated in this paper. When a Nafion membrane is embedded into a PEMFC and this is put into operation, usually the level of hydration along the membrane thickness is not uniform. The main reason is that the RH on the two faces of the membrane are significantly different (in particular, the RH is higher at the cathodic side due to the water released by the electrochemical reaction, and due to the protons releasing the water which they have dragged through the membrane due to the electro-osmotic drag phenomenon; at the anodic side, on the contrary, water is continuously dragged away by the protons moving towards the cathodic side). Even if the anodic and cathodic feeding flows into the fuel cell have the same RH, nevertheless, these feeding flows are usually not large enough to allow the assumption that the water released at the cathodic side and the water subtracted at the anodic side are negligible contributions. As a consequence, the value of RH on the anodic and the cathodic face of the membrane is different, and the water content at each membrane/gas boundary is different as well. This causes a profile of membrane humidification across the membrane thickness, which in turns is the driving force for a water diffusion flow [18]. On the contrary, in the present paper we have considered the membrane exposed to the operating conditions used for water uptake measurements [6–11] and for the proton conductivity measurements [17], i.e. the membrane is suspended in an environment at uniform and controlled temperature and relative humidity. In our model, both sides of the membrane are in identical conditions and at the same RH, and thus the membrane humidification (which is evaluated as an average of the water content of the pores of different dimensions present in the membrane itself) is the same at each gas/membrane interfaces and also throughout the whole membrane, and thus no water diffusion is expected to take place. In addition, in PEMFCs the number of water molecules dragged by the protons along the membrane due to the electro-osmotic drag phenomenon varies along the membrane thickness since it depends on the local value of the membrane hydration [18]; the number of water molecules dragged by the protons is lower in the regions where membrane hydration is poorer. This is a further mechanism of water transport through the membrane since in this way, for example, if protons move from a region at high humidity to a region at low humidity, they transport water from the previous to the latter region. This effect is not considered in the present model since, as explained above, the hydration level of the membrane is uniform through the whole membrane.

Thus, the model presented in this paper does not include water diffusion and the electro-osmotic drag, since, in the operating conditions considered here, the first is not expected to occur and the second is not expected to have an effect. For the purposes of PEMFC simulation, the present model can be coupled to the model of water diffusion and electro-osmotic drag through the membrane.

2. Model formulation

The model, starting from a pore size distribution of the Nafion® membrane, evaluates the occurrence of capillary condensation in the pores of the membrane, calculates their proton conductance and finally the overall proton conductivity of the membrane taking into account percolation within the pore network through the effective medium approximation. The model is structured as depicted in Fig. 3. In the following, each step is described in detail.

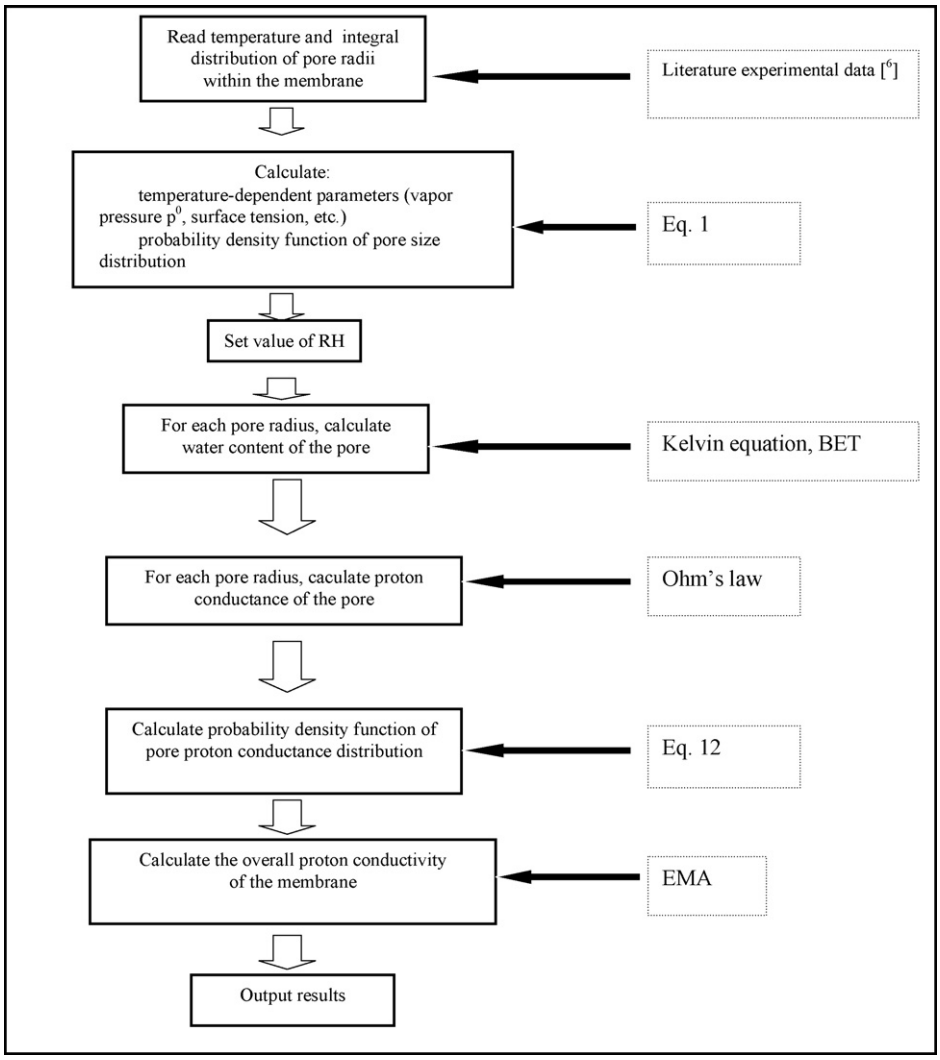

Fig. 3. Flow chart of the computational algorithm.

2.1. Pore size distribution

The pore size distribution of a Nafion® 117 membrane has been evaluated experimentally by Divisek et al. [6], by means of a method of standard porosimetry. In this method (which is considered by some scientists more suitable for ridged materials, such as the gas diffusion layer, than for membranes), they were able to obtain curves representing the integral pore volume-fraction distribution v (expressed as $cm^3\ cm^{-13}$ of overall membrane volume), in terms of radii for Nafion® 117 membranes at 20 and 80 °C; the data at 20 °C are reported in Fig. 4. The meaning of the experimental points is that $v_{i+1} - v_i$ is the overall volume-fraction of all the pores having radius ranging between r_i and r_{i+1}. Under the assumption that all the pores have the same length (which is also the basic assumption behind the Effective Medium Approximation theory, see section below), the number of pores having a certain radius r is proportional to their overall volume divided by r^2; thus, the experimental curves of v can be used to obtain the pore probability density by

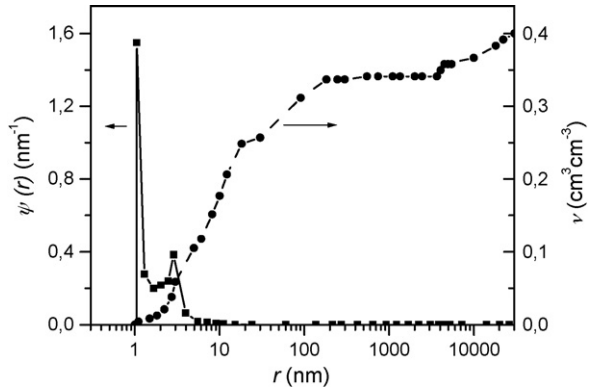

Fig. 4. (■) Probability density function of pore radius distribution $\psi(r)$ for Nafion® 117 at 20 °C, derived from (●) literature experimental data of integral pore volume distribution v at 20 °C [6].

applying the following equation to the experimental points:

$$\tilde{\psi}\left(\frac{r_i + r_{i+1}}{2}\right) = \left(\frac{2}{r_i + r_{i+1}}\right)^2 \frac{v_{i+1} - v_i}{r_{i+1} - r_i} \quad (1)$$

The resulting probability density function $\psi(r)$ is then obtained by linearly connecting the points obtained and normalizing the area to 1. The results obtained for the probability density function evaluated at 20 °C are reported in Fig. 4; it can be noticed that it is very narrow, with no pores below 1.05 nm and above about 10 nm. Also, it displays a bimodal behaviour with two peaks, respectively at 1.05 and 2.9 nm. This picture of the membrane pores is in quite good agreement with previous literature results, such as ones reported by Gierke et al. [1], which proposed a widely accepted description of the polymeric membrane in terms of an inverted micellar structure in which the ion exchange sites separate from the fluorocarbon backbone thus forming clusters (pores); they reported that when the membrane is in the dry form, an average cluster has a radius of about 1.8 nm.

2.2. Capillary condensation in Nafion® pores

The isotherm reported in Fig. 5 is referred to as 'Type IV' isotherm [14]. It is characteristic of some particular types of porous solids and it is generally accepted that it appears only in solids that have pore diameters ranging from tens to hundreds of Angstrom units. Indeed, after the physical adsorption process (branch AB in Fig. 5), that is identical for both adsorption and desorption branches, a differentiation occurs between adsorption and desorption branches. In the adsorption branch, capillary condensation occurs (branch BCE in Fig. 5) due to instability of the film interface due to the wall curvature arising for an overall adsorption layer of thickness t in pores of radius r. This causes water condensation in liquid-like conditions leading to complete obstruction of the pores of radius r. This phenomenon is referred to as capillary condensation; the classical theoretical approach used to describe it is the Kelvin–Cohan equation for adsorption [19]:

$$RT\ln(\mathrm{RH}) = -\frac{\gamma V_\mathrm{L}}{r_\mathrm{c} - t} \quad (2)$$

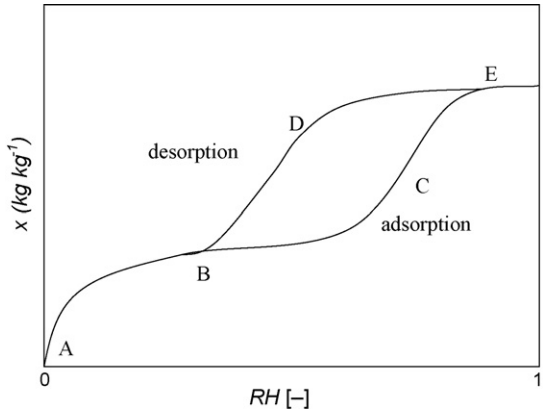

Fig. 5. Type IV isotherm of porous solids (IUPAC classification, [14]).

where γ is the surface tension, V_L the molar volume of the bulk liquid and r_c is the pore of the 'critical' radius: pores with radii below r_c are completely flooded with water. Capillary condensation is characterized by hysteretical behaviour, since evaporation/desorption follows a different mechanism (branch EDB in Fig. 5), related to the formation of a meniscus between the condensed fluid and the vapour, which stretches across the pore; in this case, the fluid on to the pore walls can be assimilated to a layer of thickness t and follows the Kelvin–Cohan equation for desorption [19]:

$$RT\ln(\mathrm{RH}) = -\frac{2\gamma V_\mathrm{L}}{r_\mathrm{c} - t} \quad (3)$$

In Eqs. (2) and (3), the value of t can be expressed as a function of RH through the following equation [14]:

$$t = \left(\frac{x}{x_\mathrm{m}}\right)\sigma \quad (4)$$

where σ can be assumed to be the molecular diameter of the adsorbate (for water, $\sigma \approx 3$Å), and x/x_m is given by the modified BET equation (see Eqs. (6) and (7)).

Even if the Kelvin–Cohan equations are slightly approximated for pores smaller than 20 nm [14,20], they are still currently applied in a number of applications, and for example they constitute the basis for the Barrett–Joyner–Halenda (BJH) method for the pore size distribution analysis, which is implemented as the standard technique on all automated commercial adsorption instruments.

2.3. Water adsorption in Nafion® pores

The process of gas/vapour adsorption in porous solids and membranes has been extensively studied [14,20,21], and is the basis of experimental techniques leading to the estimation of pore size distribution and specific surface area. In the general case of a non-polar adsorbate and a porous solid with no ionogenic groups, the process occurring at low partial pressures of the adsorbate in the gas phase in thermodynamic equilibrium with the porous solid is the physical adsorption. Physical adsorption is defined as the condensation of gases on free surfaces [14] and is considered to involve as a first step in the formation of a monolayer, i.e. a completely filled single layer of adsorbate molecules accommodated on the accessible internal surface of the porous solid. By increasing the partial pressure of the adsorbate in the gas phase, further layers start to build up on to the first monolayer (multilayer adsorption). The equation generally used to describe multilayer adsorption in porous solids is the Brunauer–Emmet–Teller (BET) equation, which is derived from a kinetic approach to the process of adsorption:

$$\frac{x}{x_\mathrm{m}} = \frac{c(p/p^0)}{(1 - p/p^0)[1 + (c-1)p/p^0]} \quad (5)$$

where x is the specific mass of the adsorbed gas, x_m the specific mass of the adsorbed gas on the monolayer and c is a parameter related to the molar enthalpy of adsorption. c and x_m are usually treated as fitting parameters, which are evaluated by fitting the experimental data of adsorption through Eq. (5).

However, when the adsorbate is a polar molecule (as water) and ionogenic groups are present in the membrane, the process of adsorption is primarily due to solvation of the membrane ionogenic groups, and the BET equation is not applicable *tout court*. As reviewed by Freger et al. [22], in this case several approaches have been used to obtain an analytical equation for the water uptake as a function of water activity, that is the water sorption isotherm. Indeed, the BET equation has been applied, under the hypothesis of treating the phenomenon of ion solvation as a typical adsorption process, but it has been demonstrated to be reliable only for low activities, up to ~0.3. Other equations have been proposed and among them the modified BET equation has been demonstrated to be suitable for the whole range of activities spanning from 0 to 1. This model is widely applied and commonly accepted for the interpretation of isotherms of water adsorption in hydrophilic polymers [22]. It is based on the consideration that the activity appearing in the BET equation must be multiplied by an 'activity coefficient' k, which accounts for the particular type of water–water interaction in the various solvation layers. Thus, the modified BET equation reads as follows:

$$\frac{x}{x_m} = \frac{ck(p/p^0)}{(1-kp/p^0)[1+(c-1)kp/p^0]} \quad (6)$$

where the number of fitting parameters is three; the physical meaning of the parameters x_m and c is, in principle, the same as that of the BET equation.

Considering the experimental points reported in Fig. 2, the branches of the adsorption and desorption curves which superimpose can be considered as the branches where only adsorption/desorption occurs, and thus that part has been interpolated through the modified BET equation, rewritten as follows:

$$\frac{\lambda}{\lambda_m} = \frac{ck(p/p^0)}{(1-kp/p^0)[1+(c-1)kp/p^0]} \quad (7)$$

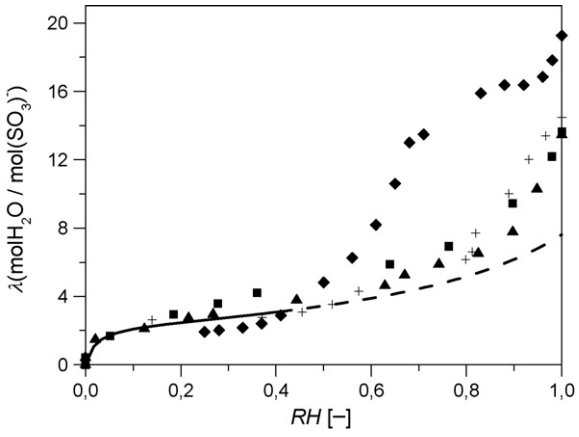

Fig. 6. (—) Interpolation of experimental literature data of water adsorption and desorption isotherms for Nafion® 117 at 20–30 °C in the region of superimposition, through the modified BET equation (Eq. (7)); (▲) adsorption at 25 °C [8]; (■) adsorption at 25 °C [7]; (+) adsorption at 30 °C [9]; (♦) desorption at 20 °C [6].

Table 1
Value of model parameters

Model parameters (at 20 °C)	Value
l	21.5 nm
V_L	18 g mol^{-1}
γ	73 dyn cm^{-1}
κ	2.38 S cm^{-1}
σ	3 Å
λ_m (Eq. (7))	2.3 mol(H_2O)/mol (SO_3^-)
c (Eq. (7))	70
k (Eq. (7))	0.7

Fig. 6 reports the results of the interpolation; the values of the parameters λ_m, c, k derived from a least square fitting method are reported in Table 1.

2.4. Evaluation of proton conductance of the pores

The model is based on the hypothesis that proton conduction occurs within the water contained in each pore of the Nafion® membrane. This approach is proposed and followed by a number of researchers [5] (more comprehensive approaches are reviewed in [23]). Thus, a simplified evaluation of the proton conductivity of the water contained in the pores of the membrane can be made, based upon the evaluation of the concentration of protons into the water contained in the membrane pores, which, in turn, is obtained on the basis of the equivalent weight of the membrane (EW = 1100 g mol^{-1}), the density of the dry membrane (ρ_{memb} = 2.24 g cm^{-3}) and of the overall volume-fraction of the pores of the membrane ($v \approx 0.4$, see Fig. 4), in the following way:

$$C = \frac{\rho_{memb}}{v \cdot EW} \quad (8)$$

The concentration calculated in this way is C = 5.1 M. Under these conditions of high concentration, the molar conductivity can be assimilated to the limit molar conductivity of protons in water, which is $\Lambda_m^0 = 350$ S cm^2 mol^{-1} at ambient temperature [24]. Thus the conductivity, calculated as:

$$\kappa = \Lambda_C^0 C \quad (9)$$

is 2.38 S cm^{-1} at 20 °C. This value is then used to calculate the conductance of each pore, keeping in mind that for every value of the relative humidity the water content of each pore depends on the pore radius. For pores with radius smaller than the critical radius r_c, satisfying the Kelvin–Cohan equation (Eq. (2)) water condensation in liquid-like conditions leads to complete obstruction of the pores. Thus, for a given temperature and relative humidity, all the pores having radius smaller than r_c are completely filled with water, while pores having a radius larger than r_c only have their walls covered by a water layer, as depicted in Fig. 7. The thickness of the water layer in pores is calculated from Eq. (4), where σ is the molecular diameter of water.

Under these conditions, once the water content of each pore is calculated, its proton conductance is easily evaluated by applying Ohm's law. For a pore completely filled with water, the

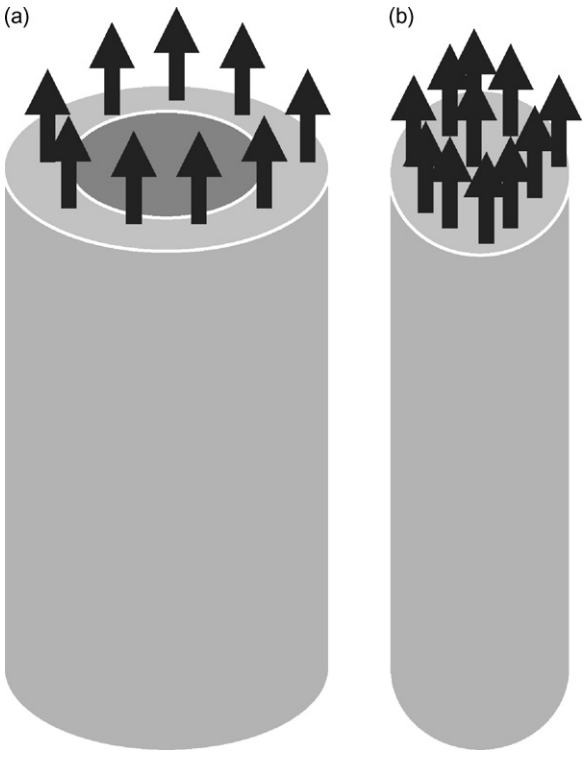

Fig. 7. Schematisation of pores with different degrees of water filling: (a) surface adsorption ($r > r_c$); (b) capillary condensation ($r \leq r_c$). Arrows represent protons.

proton conductance g is:

$$g = \kappa \frac{\pi r^2}{l} \tag{10}$$

If only a layer is present, the following formula is applied:

$$g = \kappa \frac{2\pi r t}{l} \tag{11}$$

Actually, in order to take into account that the first layer of water molecules attached to the membrane pores are somehow bridged to the SO_3^- groups and thus not completely free to rotate and allow proton conduction, water layer thickness thinner than 3.8 Å have been considered not to contribute to the proton conduction mechanism.

Starting from the previously mentioned distribution of pore sizes, the probability density function of the conductance within the membrane is also evaluated (applying the rules for the functions of random variables):

$$\phi(g) = \frac{\psi(gl/\pi\kappa)}{\left|2\sqrt{\pi\kappa g/l}\right|} + \frac{\psi((gl/2\pi\kappa t) + (t/2))}{|2\pi\kappa t/l|} \tag{12}$$

When RH is low, the water film adsorbed on the surface walls of the pores is thin (Fig. 7a), the contribution of these pores to the overall proton conduction is small, and the proton conductivity of the membrane is based only on the transport occurring in the flooded pores (Fig. 7b). Under these conditions, connectivity among the flooded pores in the membrane is a key aspect. Indeed, when the concentration of the flooded pores is low, they are either isolated or grouped in small isolated clusters. When RH is increased, then concentration of flooded pores increases and larger clusters are formed, i.e. the mean size of clusters increases monotonically. As the concentration of flooded pores approaches the percolation threshold from below, the larger clusters begin to merge, creating a few extremely large clusters, so that at the percolation threshold the mean cluster size diverge to infinity, which means that for any size of the system (membrane) under consideration, there is a complete path of adjacent flooded pores crossing the membrane, and thus macroscopic proton flow becomes possible.

2.5. Simulation of the pore network through the effective medium approximation (EMA)

The EMA has been used in order to evaluate the conductivity of the disordered pore structure within the membrane. This method was first proposed to evaluate the electrical permittivity of a binary random mixture of continuous phases [25], and later on it has been applied to the evaluation of the conductivity of random conductor networks [26,27]. In this approach, the disordered medium is replaced by a uniform system (Fig. 8) whose properties are described by an analytical equation [26,27]:

$$\int_{g_a}^{g_b} \frac{(g_M - g)\,\phi(g)}{g + (n_T/2 - 1)\,g_M} dg = 0 \tag{13}$$

Eq. (13) allows the evaluation of the effective conductance g_M of the uniform system consisting of nodes, each connected to its neighbours by a number of conducting elements n_T (=2,3,4, ... ∞), having conductance $g_a \leq g \leq g_b$; g varies randomly according to a probability density $\phi(g)$. Finally, the effective conductance g_M evaluated for the uniform system is also an estimate for the property of the starting disordered medium. The EMA has been demonstrated to be very accurate if the system is far from the percolation threshold, regardless of the expression used for $\phi(g)$ (however, the EMA predictions may be less accurate close to the percolation thresholds) [28].

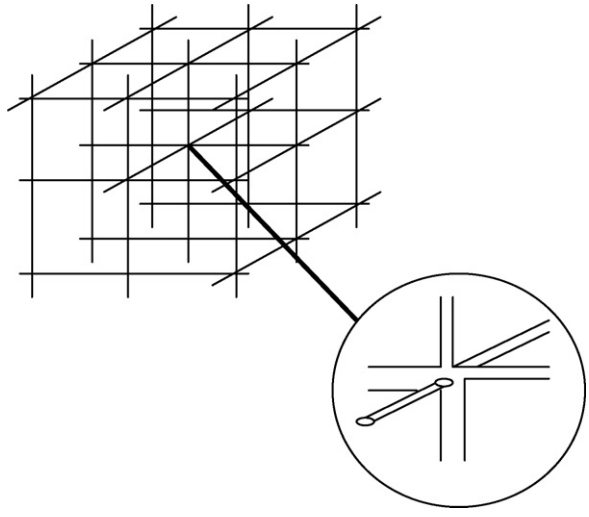

Fig. 8. Schematisation of a three-dimensional cubic pore network ($n_T = 6$) conforming to the EMA assumptions.

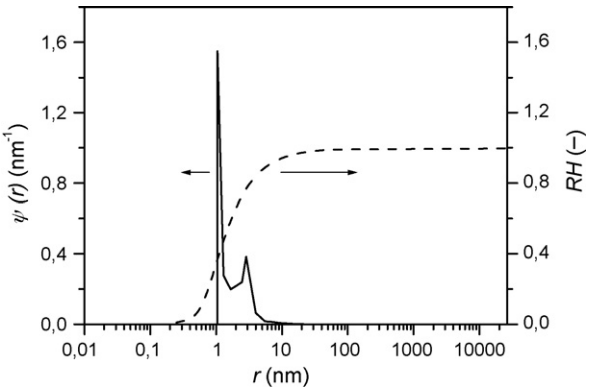

Fig. 9. (—) Probability density function of pore radius distribution data for Nafion® 117 at 20 °C (extracted from [6]). (- - -) Calculation of the relative humidity RH in correspondence of which a certain radius becomes critical for capillary condensation at 20 °C.

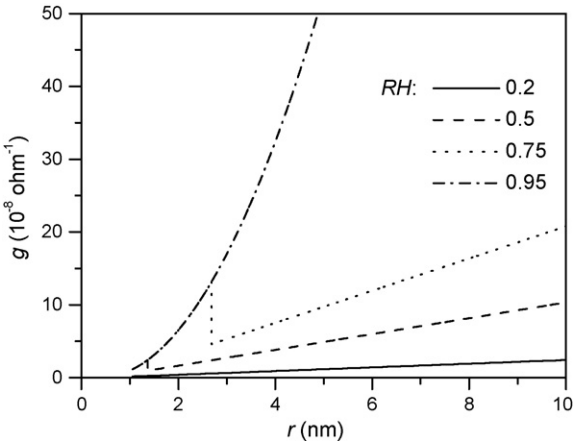

Fig. 10. Pore conductance g as a function of pore radius r in Nafion® 117 at 20 °C for various values of relative humidity RH.

2.6. Pore length estimation

The evaluation of the pore size distribution has also allowed estimation of the typical pore length; indeed, conforming to the assumptions made for the EMA, by assimilating the pore network structure to a regular cubic network, the following equation applies:

$$\frac{3\int_{r_{\min}}^{r_{\max}} \pi r^2 \psi(r)\mathrm{d}r}{l^2} = \varepsilon \tag{14}$$

Considering that the void degree of the membrane is about $\varepsilon \approx 0.4$ (see also Fig. 4), the estimated pore length is about 20 nm.

3. Results and discussion

The model is independent on membrane thickness, and thus the results presented in this section hold for Nafion® membranes of any type (111, 112, 115, 117, etc.), provided that their pore size distribution is the same as that used in this paper [6], which was obtained specifically from Nafion® 117 membranes.

Fig. 9 reports the probability density function of pore radius distribution for a Nafion® 117 membrane at 20 °C; the same figure also shows the relative humidity RH in correspondence of which a pore having a certain radius becomes completely

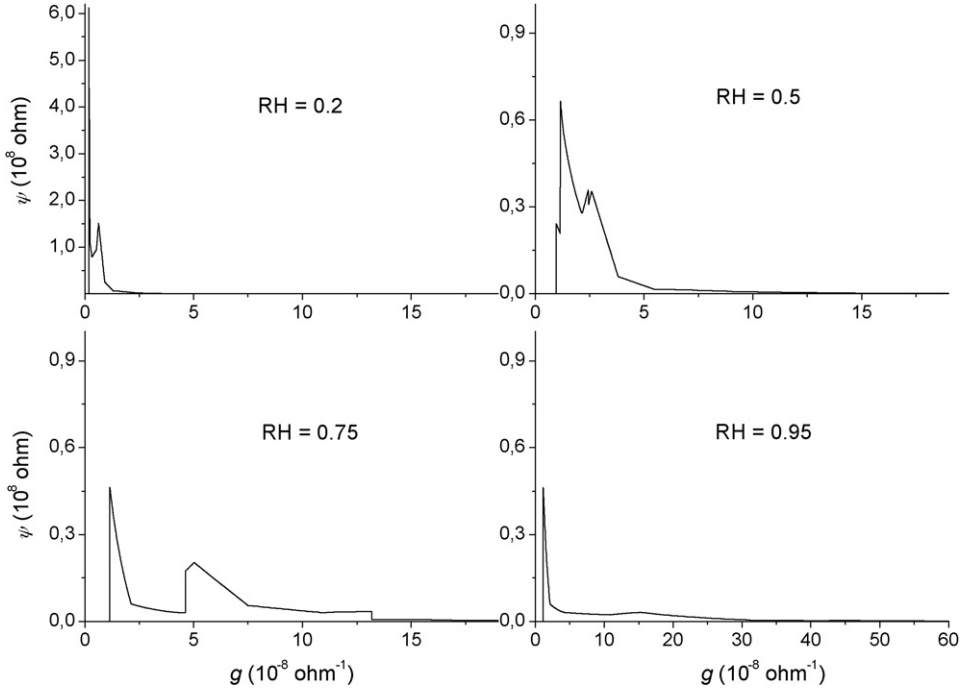

Fig. 11. Model results of probability density of pore proton conductance g in Nafion® 117 at 20 °C at different values of relative humidity RH.

flooded due to capillary condensation (according to Eq. (2)). Fig. 9 shows that the smallest pores of the membrane (radius of 1.05 nm) become completely flooded with water at a relative humidity of about 0.37, which is therefore the starting point for the occurrence of capillary condensation. It is interesting to note that this is in quite good agreement with what is displayed in Fig. 2, showing that divergency between the adsorption and desorption isotherms, which is again the starting point for capillary condensation, occurs approximately for the same RH.

Thus, in the model, for RH < 0.37, no condensation occurs in the pores of the membrane, and only water adsorption on to the surface of the pore walls takes place. Thus, proton conductivity occurs only in the thin water layers adsorbed on to the pore walls, and its value is relatively small (see the curve representing the conductance g obtained at RH = 0.2 reported in Fig. 10). On the contrary, when RH reaches 0.37, capillary condensation starts occurring in the smallest membrane pores, with radius of about 1.05 nm. When RH is increased above 0.37, the curve representing the proton conductance g presents two regions, which are clearly visible in Fig. 10 for the curve obtained at RH = 0.75: in the first region, for small pore radii ($0 < r < 2.7$ nm) the pores are completely filled with liquid water, and their conductance increases quadratically as a function of the pore radius according to Eq. (10), reaching the maximum value of $1.3 \times 10^{-7}\ \Omega$ for a pore radius of 2.7 nm; for pore radii larger than 2.7 nm, which is the critical radius for capillary condensation at RH = 0.75, there is a sharp decrease in conductance, due to the fact that the pores are no more filled with liquid water. From 2.7 nm onwards, the conductance increases linearly with the pore radius (Eq. (11)), and for large pore diameters (around 10 nm) the conductance is quite remarkable again, since these pores, even if still empty in their middle, have a significant amount of water adsorbed on to their wall surface. In Fig. 10, this type of behaviour is visible for the curves representing conductance versus pore radius obtained at RH = 0.75, but also for RH = 0.6 (in this case the critical radius for capillary condensation is about 1.4 nm), while for RH = 0.95 the critical radius is about 11.6 nm, and therefore all the pores in the range represented in the figure are completely filled with water, and the sharp transition corresponding to r_c is not displayed in the figure.

Correspondingly, the plots of $\psi(g)$ reported in Fig. 11 show that the probability density is concentrated for very low values of conductance for RH = 0.2, where it displays a bimodal shape, very similar to the shape of the pore size distribution. $\psi(g)$ shifts towards larger values of conductance by increasing RH; indeed, for RH = 0.5, $\psi(g)$ shows a primary peak for values of conductance of about $1.15 \times 10^{-8}\ \Omega$, corresponding to the most probable pore sizes (1.05 nm) getting completely filled up with liquid water. The same peak also remains unchanged at RH = 0.75 and RH = 0.95. All the distributions also show a secondary peak; this secondary peak represents the conductance of the secondary peak of the pore size distribution, and, due to its gradual filling up with water due to capillary condensation, it gradually moves towards higher values of conductance as RH is increased, as represented in the curves for RH = 0.75 and RH = 0.95 of Fig. 11.

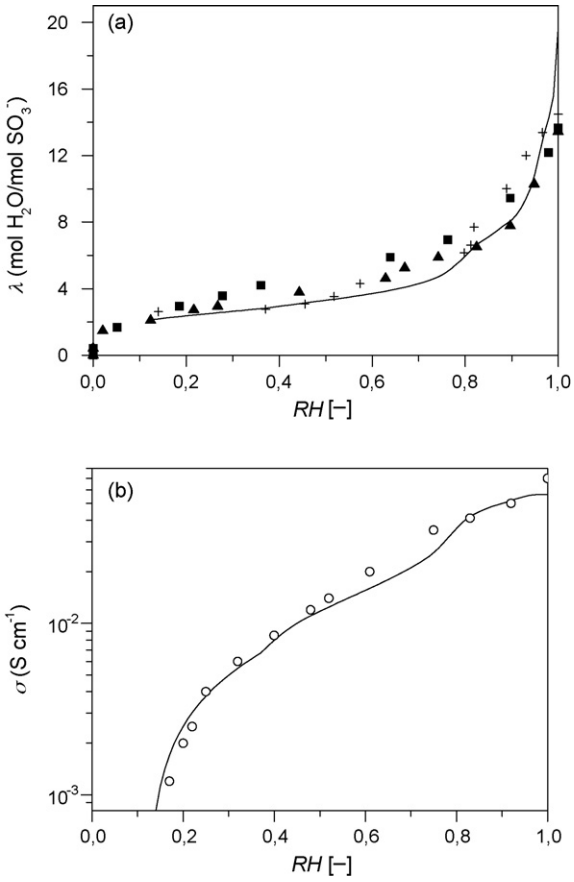

Fig. 12. Simulation of Nafion® 117 at 20 °C. Comparison between model results (lines) and literature experimental data (symbols). (a) Adsorption isotherms (experimental data as in Fig. 2); (b) proton conductivity (experimental data from [17]).

Fig. 12a displays the results obtained from the present model in terms of water adsorption for a Nafion® 117 membrane at 20 °C (the water desorption branch of the isotherm has not been simulated since, due to the occurrence of the Schroeder paradox, two different values of water uptake are obtained experimentally for RH = 1, which cannot be obtained by the model). The agreement between simulation data and experimental literature reported in Fig. 12a is good. In parallel, the conductivity of the membrane has also been calculated, and the results are reported in Fig. 12b together with experimental literature data; the agreement is also good in this case.

Fig. 12 shows how the membrane water uptake and the membrane conductivity increase when increasing the RH. It is interesting to note that, even if for RH = 0.75 most of the pores of the membrane are completely filled with water, no 'level off' situation is reached for the average membrane conductivity (please note that the y-scale of Fig. 12b is logarithmic). This is due to the fact that, even if at RH above 0.75 there is a very small number of pores which are still empty, nevertheless, those pores are the largest ones, and thus, when filled with water, they give a significant increment to the overall conductivity. This is displayed by Fig. 12, which shows a continuous increase in conductivity up to RH close to 1.

The model can also be applied to higher operating temperatures (in any case, below 100 °C at the operating pressure of 1 atm); since the pore size distribution of Nafion® membranes changes with temperature, a proper pore size distribution needs to be known for the operating temperature under consideration.

4. Conclusions

In this paper, a model is proposed for the simulation of Nafion® proton conductivity, where it is assumed that, when starting from a dry membrane and by increasing RH, membrane pore-filling is due to water adsorption on the pore walls coupled to capillary condensation; for each value of RH, some of the pores (the smallest ones) are completely filled with water, while the largest pores contain only a thin layer of water adsorbed on their pore surface. The conductance of each pore is thus very different depending on its radius, and the overall conductivity of the membrane depends on the percolation through the pore network. In this paper, a model of Nafion® membranes is proposed, which, starting from literature data for the pore size distribution [6], evaluates the occurrence of capillary condensation in the pores of the membrane, calculates their proton conductance, and finally the overall proton conductivity of the membrane taking into account percolation within the pore network through the effective medium approximation.

The simulation results of proton conductivity of a Nafion® 117 membrane at 20 °C show good agreement with literature experimental data, even when varying the RH operating conditions.

The model is independent of membrane thickness, and thus the results presented in this paper hold for Nafion® membranes of any type, provided that their pore size distribution is the same as that used in this paper [6], which was obtained specifically from Nafion® 117 membranes. The model can also be applied to higher operating temperatures (in any case, below 100 °C at the operating pressure of 1 atm); since the pore size distribution of Nafion® membranes changes with temperature, a proper pore size distribution needs to be known for the operating temperature under consideration.

This type of model could be applied (provided that the pore size distribution is known) also to other proton conducting polymers formed by a backbone with sulphonic groups (or other protogenic groups) linked, such as those polymers synthesised by the Dow Chemical Company and the Asahi Chemical Company.

References

[1] T.D. Gierke, W.Y. Hsu, in: A. Eisenberg, H.L. Yeager (Eds.), Proceedings of the ACS Symposium on Perfluorinated Ionomer Membranes, ACS Symposium Series No. 180, American Chemical Society, Washington, DC, 1982, pp. 283–315.
[2] M. Eikerling, A.A. Kornyshev, A.M. Kuznetsov, J. Ulstrup, S. Walbran, J. Phys. Chem. B 105 (2001) 3646–3662.
[3] S. Walbran, A.A. Kornyshev, J. Chem. Phys. 114 (2001) 10039–10048.
[4] T. Okada, G. Xie, O. Gorseth, S. Kjelstrup, N. Nakamura, T. Arimura, Electrochim. Acta 43 (1998) 3741–3747.
[5] E. Spohr, P. Commer, A.A. Kornyshev, J. Phys. Chem. B 106 (2002) 10560–10569.
[6] J. Divisek, M. Eikerling, V. Mazin, H. Schmitz, U. Stimming, Yu.M. Volfkovich, J. Electrochem. Soc. 45 (1998) 2677–2683.
[7] K.K. Pushpa, D. Nandan, R.M. Iyer, J. Chem. Soc., Faraday Trans. 1 (84) (1988) 2047.
[8] D. Morris, X. Sun, J. Appl. Polym. Sci. 50 (1993) 1445–1452.
[9] T.A. Zawodzinski, C. Deruin, S. Radzinski, R.J. Sherman, V.T. Smith, T.E. Springer, S. Gottesfeld, J. Electrochem. Soc. 140 (1993) 1041–1047.
[10] J.T. Hinatsu, M. Mizyhata, H. Takenata, J. Electrochem. Soc. 141 (1994) 1493.
[11] C.M. Gates, J. Newman, AIChE J. 46 (2000) 2076–2085.
[12] N. Cornet, G. Gebel, J. Phys. IV France 8 (1998) 63–68.
[13] N.H. Jalani, P. Choi, R. Datta, J. Membr. Sci. 254 (2005) 31–38.
[14] S.J. Gregg, K.S.W. Sing, Adsorption, Surface Area and Porosity, Academic Press, London and New York, 1982.
[15] P. Rajniak, M. Soós, R.T. Yang, AIChE J. 45 (1999) 735–750.
[16] F. Štěpánek, M. Marek, P.M. Adler, AIChE J. 45 (1999) 1901–1911.
[17] Y. Sone, P. Ekdunge, D. Simonsson, J. Electrochem. Soc. 143 (1996) 1254–1259.
[18] T.E. Springer, T.A. Zawodzinski, S. Gottesfeld, J. Electrochem. Soc. 138 (1991) 2334–2342.
[19] L.H. Cohan, J. Am. Chem. Soc. 60 (1938) 433–435.
[20] A.V. Neimark, P.I. Ravikovitch, Micropor. Mesopor. Mater. 44/45 (2001) 697–707.
[21] Y.C. Yortsos, A.K. Stubos, Curr. Opin. Colloid Interface 6 (2001) 208–216.
[22] V. Freger, E. Korin, J. Wisniak, E. Korgold, J. Membr. Sci. 128 (1997) 151–162.
[23] K.-D. Kreuer, S.J. Paddison, E. Spohr, M. Schuster, Chem. Rev. 104 (2004) 4637–4678.
[24] A.A. Kornyshev, A.M. Kunetsov, E. Spohr, J. Ulstrup, J. Phys. Chem. B 107 (2003) 3351–3366.
[25] D.A.G. Bruggeman, Ann. Phys. (Leipzig) 24 (1935), 636–644, 665–679.
[26] S. Kirkpatric, Phys. Rev. Lett. 27 (1971) 1722–1725.
[27] S. Kirkpatric, Rev. Mod. Phys. 45 (1973) 574–588.
[28] M. Sahimi, Applications of Percolation Theory, Taylor & Francis, London, 1994.